

Meshless Analysis of Casting Process Considering Non-Fourier Heat Transfer

A. Khosravifard* and M. R. Hematiyan

Department of Mechanical Engineering, Shiraz University, Shiraz, Iran

Abstract: Casting is considered as a major manufacturing process. Thermal analysis of a solidifying medium is of great importance for appropriate design of casting processes. The conventional governing equation of a solidifying medium is based on the Fourier heat conduction law, which does not account for the phase-lag between the heat flux and the temperature gradient. In this paper, the concept of phase-lag during the phenomenon of solidification is investigated. This concept is considered by utilization of the hyperbolic heat conduction equation, known generally as the Maxwell–Cattaneo relation. In this way, the effect of finite heat wave speed on the thermal behavior of a solidifying medium is studied. In this context, some numerical example problems are analyzed with the meshless radial point interpolation method. The effect of the relaxation time on the thermal behavior of the solidifying medium is investigated. Moreover, the results of Fourier and non-Fourier heat conduction equations are compared. It is observed that based on the specific solidification process and the amount of relaxation time, the results of the Fourier and non-Fourier conduction laws can be quite different. The most prominent effect of the relaxation time is to alter the initiation of the solidification at each point.

Keywords: Phase-change, non-Fourier heat conduction, meshless radial point interpolation method

1. Introduction

The phenomenon of heat transfer accompanied by the change of phase is known as solidification or melting. The phase-change problems are accompanied by the liberation or absorption of energy. A moving interface exists between the two phases of material, with an abrupt difference in thermo-physical properties of the matter on the sides of the interface. Therefore, such problems are usually referred to as the moving boundary problems. Phase change problems are important to many engineering applications such as materials processing, purification of metals, growth of pure crystals from melts and solutions, solidification of castings and ingots, welding, electroslag melting, zone melting, thermal energy storage, ice making, aerodynamic ablation, and many other applications.

Numerous research works can be found in the literature that deal with the analytical as well as numerical analysis of the solidification problems. Due to the complicated nature of the solidification phenomenon, for most practical cases no analytical solutions can be found. Consequently, the numerical methods are usually the only available tool for the analysis of such problems. Among the numerical methods, meshless techniques are best suited for the analysis of moving boundary problems [1]. Vertnik and Sarler [2] developed a new local radial basis function collocation method (LRBFCM) for the analysis of solid-liquid phase change systems. Later, Kosec and Sarler [3] applied the mentioned method to the analysis of coupled heat transfer and fluid flow problems with solid-liquid phase change. In that work, the problem of melting/freezing of a pure substance was solved in primitive variables on a fixed grid with convection suppression, proportional to the amount of the solid fraction. Vertnik et al. [4] used an upgrade of the classical meshless Kansa method for the solution of transient heat transport in direct-chill casting of aluminum alloys. The problem was characterized by a moving mushy domain between the solid and the

liquid phases and a moving starting bottom block that emerged from the mold during the process. Zhang et al. [5] used the finite point method (FPM) for modeling metal solidification processes in continuous casting. Zhang et al. [6] used the FPM along with the meshless local Petrov-Galerkin method for numerical simulation of solidification process and evaluation of thermal stresses of continuous casting billet in mold. Zhihua et al. [7] employed the element free Galerkin (EFG) method for the analysis of heat transfer problems with phase change. The method was then utilized for solution of the thermal problem involving phase change in permafrost embankment. Smoothed particle hydrodynamics (SPH) method has been also used for the simulation of solidification process [8]. Zhang et al. [9] developed an SPH formulation for simulation of free surface and solidification problems.

More recently, Yang and He [10] presented a new smoothing method for modeling the effective heat capacity in the EFG method. They used the proposed method for the analysis of solidification problems. Alizadeh et al. [11] exploited the FPM to simulate the solidification process of continuously cast steel bloom in both primary and secondary cooling regions. To validate their results, the solidified shell thickness simulated by the FPM was compared with the solidified shell, measured on a breakout bloom. Kosec and Sarler [12] applied the LRBFCM to the solution of the freezing process with convection in the liquid phase for a metal-like material in a closed rectangular cavity. To avoid inclusion of additional boundary conditions at the fluid-solid interface, the enthalpy one-domain formulation was used. Furthermore, in order to avoid numerical instabilities, the freezing of a pure substance was modeled by a narrow phase change interval. Sarler et al. [13] developed a new meshless solution procedure for calculation of one-domain coupled macroscopic heat, mass, momentum and species transfer problems as well as phase-field concepts of grain evolution. The solution procedure was defined on the macro as well as on the micro levels by a set of nodes, which could be non-uniformly distributed. The concept and the results of the proposed multi-scale solidification modeling were compared with the classical mesh-based approach. Thakur et al. [14] discussed the application of the MLPG method to phase change problems. Apparent capacity method based on the enthalpy formulation was used in their work. Kosec et al. [15] investigated the macro-segregation as a consequence of solidification of a binary Al-4.5%Cu alloy in a 2D rectangular enclosure. Reutskiy [16] presented a meshless numerical technique for solving one and two-dimensional Stefan problems. The presented technique was based on the use of the delta-shaped functions and the method of approximate fundamental solutions (MAFS) which was originally suggested for solving elliptic problems and heat equations in domains with fixed boundaries. Vertnik and Sarler [17] solved an industrial benchmark test problem by a meshless method. In their work, a mixture continuum model was used to treat the solidification system. Kumar et al. [18] made use of the immersed boundary method for continuous casting simulation involving boundary movement. In their methodology, the immersed boundary method was coupled with the second-order accurate finite difference solution of unsteady three-dimensional heat conduction equation.

In almost all of the present works, the phenomenon of phase change is modeled by the classical parabolic diffusion energy equation. The classical diffusion energy equation is based on the Fourier law of heat conduction, which implies an immediate response for the conduction heat flux to the temperature gradient at each point. In other words, in the Fourier model, it is assumed that the heat wave propagates with an infinite speed. Less attention has been paid to applications of phase-change problem in which the heat wave propagates at a finite speed [19–21]. As an example of such applications, laser and microwave incident energy can be named which involve large temperature gradients over small time durations [22]. Other applications involve rapid freezing of tissue cells during cryopreservation. Cryopreservation is a process in which cells, whole tissues, or any other substance susceptible to damage caused by chemical reactivity or time, are preserved by cooling to sub-zero temperatures. In this process, biological systems are exposed to extremely high cooling rates (thousands of °C/min), which leads to solidification [23]. The

cryopreservation is widely used in stem cell research [24, 25], preservation of organs for transplant [26] and tissue products storage and transportation [27].

There are a limited number of works in the literature that deal with hyperbolic heat conduction during solidification. Sobolev [19] has considered a local non-equilibrium model for heat transport around melting and crystallization zone induced by ultra-fast laser irradiation. It was concluded that the local non-equilibrium effects lead to an interface temperature gradient that is steeper than expected from the classical heat conduction equation. Vedavarz et al. [20] theoretically analyzed the transient temperature distributions in laser-irradiated materials by considering a hyperbolic heat conduction model. In their study, hyperbolic non-Fourier models have been introduced to account for the finite speed of the thermal wave. Glass et al. [21] derived interface condition for hyperbolic phase change problems, which includes sensible heat at the interface, as an extension of the interface condition for standard parabolic phase-change problems. They presented the enthalpy formulation of the hyperbolic Stefan problem and it was used to numerically solve for the temperature distributions and the interface position. Siraj-ul-Islam et al. [28] proposed an improved localized radial basis functions collocation method for the numerical solution of hyperbolic partial differential equations which govern the non-Fourier heat conduction.

In the present work, the meshless radial point interpolation method (RPIM) is utilized for the analysis of non-Fourier heat transfer in the solidification process. Some typical problems are numerically solved, and the effect of finite heat wave speed on the behavior of a solidifying medium is investigated.

2. Problem Formulation

The classical parabolic heat conduction equation is based on the Fourier law of heat conduction, which states that the conductive heat flux is instantaneously proportional to the temperature gradient, i.e.:

$$q(x, t) = -k \frac{\partial T}{\partial x}(x, t) \quad (1)$$

In contrast, the hyperbolic heat conduction equation is based on the Maxwell–Cattaneo relation, which accounts for a time lag between the heat flux and the temperature gradient. This constitutive model is sometimes referred to as the non-Fourier law of heat conduction. To account for the finite heat wave speed in the non-Fourier law of heat conduction, the following heat flux model is considered:

$$q(x, t + \tau) = -k \frac{\partial T}{\partial x}(x, t) \quad (2)$$

where q is the heat flux, k is the thermal conductivity, and τ is the so-called thermal relaxation time. This constitutive law assumes that the effect (heat flux) and the cause (the temperature gradient) do not occur simultaneously. The delay between the effect and the cause in this situation is known as the relaxation time. Expansion of the heat flux in Eq. (2) with respect to time, results in the Maxwell–Cattaneo relation

$$\tau \frac{\partial q(x, t)}{\partial t} + q(x, t) = -k \frac{\partial T}{\partial x}(x, t). \quad (3)$$

Introducing Eq. (3) into the energy balance equation,

$$\rho c \frac{\partial T}{\partial t} = -\frac{\partial q}{\partial x}, \quad (4)$$

leads to the hyperbolic heat conduction equation:

$$\rho c \tau \frac{\partial^2 T}{\partial t^2} + \rho c \frac{\partial T}{\partial t} = k \frac{\partial^2 T}{\partial x^2}, \quad (5)$$

where c is the specific heat, and ρ is the mass density. Eqs. (1) through (5) are written for a one-dimensional medium, however they can be readily generalized for two-dimensional media as well. The hyperbolic heat conduction equation for a 2D domain can be written as follows:

$$\rho c \tau \frac{\partial^2 T}{\partial t^2} + \rho c \frac{\partial T}{\partial t} = \nabla \cdot (k \nabla T) \quad (6)$$

Presence of the second-order time derivative of the temperature in Eqs (5) and (6) allows for propagation of thermal disturbances with a finite velocity. This additional time derivative is sometimes called the *thermal inertia* [19]. It should be noted that the presence of the second-order time derivative makes it necessary to supplement Eq. (5) with an additional initial condition, i.e.

$$\left. \frac{\partial T}{\partial t} \right|_{(x,0)} = 0 \quad (7)$$

2.1. The hyperbolic solidification equation

The classical problem of heat flow involving a change of phase is the one-dimensional freezing problem first posed by Stefan in 1889. A material which can exist in two phases (liquid and solid) fills the half space $x \geq 0$. For times $t \leq 0$ the material is in the liquid phase at a constant temperature $T(x,0) = T_2 > T_m$, where T_m is the phase change temperature. At time $t = 0$ the temperature of the surface $x = 0$ is instantaneously lowered and maintained at $T(0,t) = T_1 < T_m$. This will cause a layer of solid to be formed adjacent to the surface $x = 0$ and as time progresses this layer will further expand. The Stefan problem is to follow the solid/liquid interface $x = X(t)$ as it moves forward. Figure 1 depicts the geometry and coordinates for such a one-dimensional solidification problem.

The thermal behavior of the system during the solidification can be described by Eq. (5) for each phase, along with an energy balance for the moving interface [22]:

$$\frac{\tau}{\alpha_s} \frac{\partial^2 T}{\partial t^2} + \frac{1}{\alpha_s} \frac{\partial T}{\partial t} = \frac{\partial^2 T}{\partial x^2}, \quad 0 < X(t) < x \quad (8)$$

$$\frac{\tau}{\alpha_l} \frac{\partial^2 T}{\partial t^2} + \frac{1}{\alpha_l} \frac{\partial T}{\partial t} = \frac{\partial^2 T}{\partial x^2}, \quad x < X(t) < \infty \quad (9)$$

$$-\rho_s L \frac{\partial X}{\partial t} - \tau \rho_s L \frac{\partial^2 X}{\partial t^2} = -k_s \left. \frac{\partial T}{\partial x} \right|_{t,X} + k_l \left. \frac{\partial T}{\partial x} \right|_{t,X} \quad (10)$$

where $\alpha = k/\rho c$ is the thermal diffusivity, L is the latent heat of solidification, and the subscripts s and l refer to the solid and liquid phase, respectively.

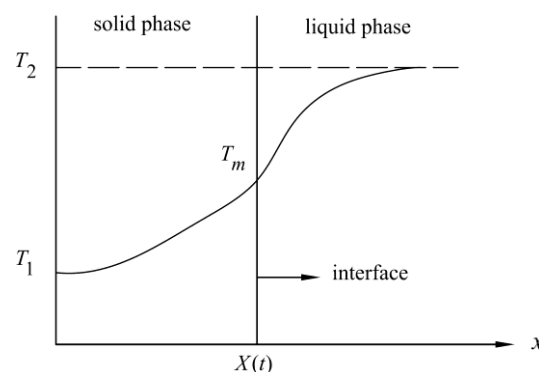


Fig. 1. The geometry and coordinates of the 1D solidification problem.

Equations (8) to (10) are the governing equations of the solidification phenomenon in a 1D medium with the concept of finite heat wave speed. These equations can be incorporated into a single equation by introducing the enthalpy function [23]:

$$\frac{\partial H}{\partial t} + \tau \frac{\partial^2 H}{\partial t^2} = k \frac{\partial^2 T}{\partial x^2}, \quad (11)$$

For 2D domains this equation reads

$$\frac{\partial H}{\partial t} + \tau \frac{\partial^2 H}{\partial t^2} = \nabla \cdot (k \nabla T) \quad (12)$$

where H is the enthalpy function or the total heat content, which for the isothermal phase change is defined as:

$$\begin{aligned} H(T) &= \int_{T_r}^T \rho c_s(T) dT & (T < T_m) \\ H(T) &= \int_{T_r}^{T_m} \rho c_s(T) dT + \rho L + \int_{T_m}^T \rho c_l(T) dT & (T \geq T_m) \end{aligned} \quad (13)$$

and for phase change occurring over a finite temperature range, the enthalpy function is written as:

$$\begin{aligned} H(T) &= \int_{T_r}^T \rho c_s(T) dT & (T < T_s) \\ H(T) &= \int_{T_r}^{T_s} \rho c_s(T) dT + \int_{T_s}^T \left[\rho \frac{dL}{dT} + \rho c_f(T) \right] dT & (T_s \leq T < T_l) \\ H(T) &= \int_{T_r}^{T_s} \rho c_s(T) dT + \rho L + \int_{T_s}^{T_l} \rho c_f(T) dT + \int_{T_l}^T \rho c_l(T) dT & (T \geq T_l) \end{aligned} \quad (14)$$

In the preceding equation, c_f is the specific heat in the freezing interval, dL/dT is the variation of latent heat in this interval, and are defined as follows, respectively:

$$c_f = \left[\frac{T - T_s}{T_l - T_s} \right] (c_l - c_s) + c_s \quad (15)$$

$$dL/dT = L/(T_l - T_s) \quad (16)$$

In Eqs (14) through (16) T_s is the solidus temperature, and T_l is the liquidus temperature.

In the present work, the meshless RPIM [29, 30] is used for the solution of governing equation of solidification with finite heat wave speed. Since the solidification problem is inherently transient, the numerical solution of the discretized system of equations is carried out by standard time integration techniques. In this paper, the Crank-Nicolson scheme is used, which is unconditionally stable. That is, irrespective of the time step size, the results are stable. Additionally, because the solidification process is nonlinear, the system of equations should be solved iteratively. This means that the time step size in each step of the analysis is varied to obtain a converged solution. Therefore, in the present approach both the stability and convergence of the solution is guaranteed.

3. Numerical Examples, Results, and Discussion

In this section, two typical numerical examples of solidification process are presented. The phase change problem in both examples is analyzed by the Fourier as well as non-Fourier heat conduction law. Different

phase lag times are considered in order to investigate its effect on the solidification process. In the first example, solidification of a semi-infinite region is investigated by considering a one-dimensional computational model. The second example deals with a common solidification process, i.e. the continuous casting. For both models a generic material is considered in the analyses.

3.1. Example 1: solidification of a semi-infinite region

As the first example, a 1D solidification problem in a semi-infinite region is analyzed by the meshless RPIM. The problem geometry is shown in Fig. 1. Both the parabolic and hyperbolic heat conduction equations are utilized for the analysis of the problem and the results are compared. In the case of the hyperbolic heat conduction, three different relaxation times are selected to investigate its effect on the thermal behavior of the solidifying medium.

For numerical modeling of the problem domain, the infinite region is represented by a finite domain, extending from $x = 0$ to $x = 1$, and the problem domain is modeled by 160 regularly spaced nodes. For obtaining numerical solutions of the one-dimensional solidification problem, the following generic data in SI units are used:

$$\begin{aligned} T_s &= -0.1; \quad T_l = 0.1; \quad T(x,0) = 0.1 \quad (x \geq 0); \\ T(0,t) &= -1; \quad T(\infty,t) = 0.1; \quad k_s = k_l = 1; \\ c_s &= c_l = 1; \quad \rho_s = \rho_l = 1; \quad L = 0.25; \end{aligned} \quad (17)$$

Figure 2 depicts the temperature variation with respect to time at $x = 0.25$ m. In this figure, the results of parabolic and hyperbolic heat conduction equations are compared. The results obtained by considering two different relaxation times, i.e. $\tau = 0.75$ and $\tau = 1.5$ msec, are depicted in this figure.

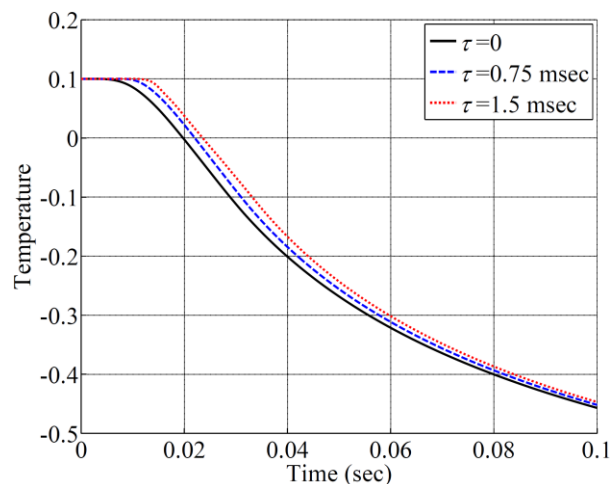


Fig. 2. Time history of temperature at $x = 0.25$ m, example 1.

Expectedly, as the relaxation time increases, so does the deviation of temperatures obtained by the parabolic and hyperbolic equations. Fig. 2 implies that the temperatures obtained by considering Fourier and non-Fourier heat law have a greater discrepancy at the beginning of the solidification progress. As time progresses the difference between the predicted temperatures of the two methods decreases.

Another observation from Fig. 2 is that the value of temperature at each instant of time increases as the relaxation time becomes greater. This is due to the amount of time lag in the diffusion of thermal wave. In the case with larger relaxation time, it takes more time for the heat wave to reach a point, and therefore, the solidification occurs at a larger instant of time.

Figure 3 depicts the time history of temperature at $x = 0.15$ m. This figure shows the same characteristics as those of Fig. 2. However, since the position of the point under investigation is now

closer to the boundary, the intensity of the heat flux is larger. As a result, the effect of the relaxation time on the results is more than the previous case. By comparing the two figures, it is observed that the deviation of the results of the hyperbolic equation from the parabolic equations is larger for the points, which are closer to the boundary.

Figure 4 depicts the position of the solidification front versus time. In this figure, the results obtained by considering three different values of relaxation time are presented. This figure clearly demonstrates the concept of time lag during solidification. The relaxation time causes the solidification front to lag behind. This means that when the concept of relaxation time is introduced in the governing equations of the solidification, the heat wave travels at a lower speed in comparison with the classical heat conduction equation.

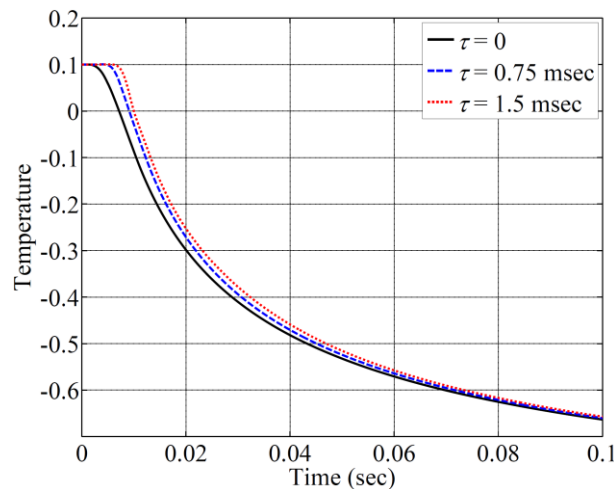


Fig. 3. Time history of temperature at $x = 0.15$ m, example 1.

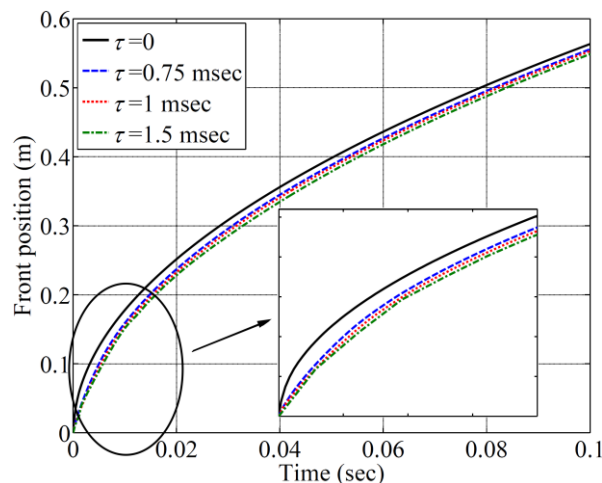


Fig. 4. Solidification front position for different values of relaxation time.

The temperature distribution within the problem domain at two instants of time is plotted in Fig. 5. This figure depicts the temperatures obtained by different values of relaxation time. Similar observations can be made from this figure. Firstly, the effect of relaxation time on the temperature distribution at $t = 0.02$ sec is much more than that at $t = 0.04$ sec. Consequently, it is inferred that the effect of relaxation time is more important in the initial stages of solidifications. Furthermore, it is observed that due to the finite speed of heat wave, the value of temperature at each point is larger for higher relaxation times.

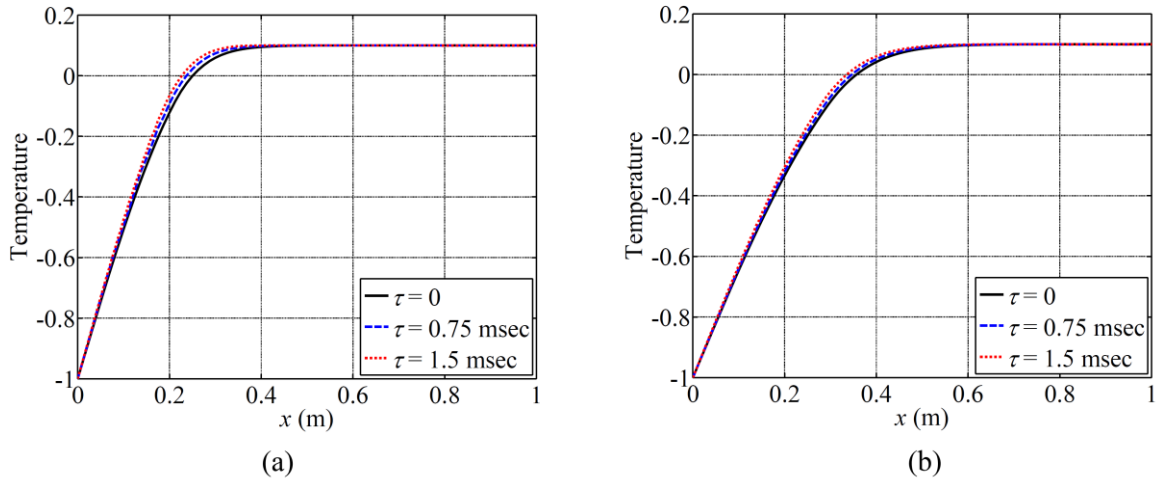


Fig. 5. Distribution of the temperature in the problem domain at (a) $t = 0.02$ sec, and (b) $t = 0.04$ sec.

3.2. Example 2: The continuous casting process

In this example, a solidification problem associated with the continuous casting process is analyzed by the meshless RPIM. The problem geometry and boundary conditions are depicted in Fig. 6. It should be mentioned that because of the symmetry of the continuous casting model, only a quarter of the problem domain is modeled and analyzed.

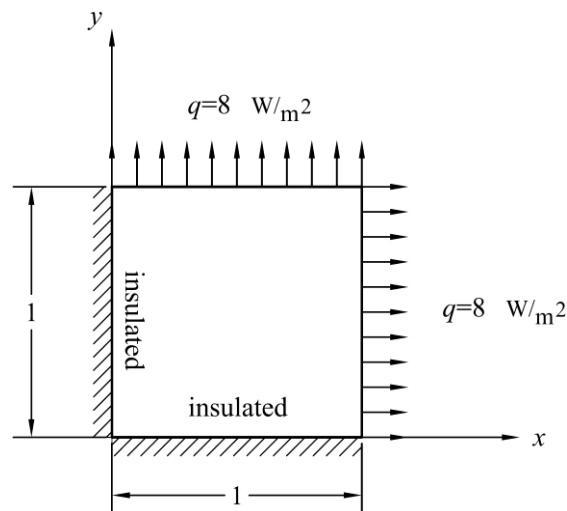


Fig. 6. Problem geometry and boundary conditions of the continuous casting process, example 2.

The material properties of this example problem are the same as those used in the previous example. The whole material is initially at $T_i = 0.1$ and the process is analyzed in a time duration of 0.1 sec. The heat flux shown in Fig. 6 accounts for all sorts of heat transfer to and from the medium, i.e. the radiative and convective heat fluxes are both accounted for in the heat flux q . Naturally, the insulated surfaces are implemented by considering a zero flux on the corresponding boundaries.

Three different relaxation times of 1, 5, and 10 msec are selected for this analysis. The problem is also analyzed by the parabolic heat conduction equation, i.e. with zero time lag. The time history of temperature for a point at $(0.5, 0.5)$ is depicted in Fig. 7. This figure compares the variation of temperature obtained by the Fourier and non-Fourier heat conduction laws. Here again, it is observed that when the relaxation time is taken into account, the solidification occurs at a later time instance.

The temporal variation of the temperature for a point closer to the cooling boundaries of the problem domain, i.e. at $(0.8, 0.8)$, is plotted in Fig. 8. From Figs 7 and 8 it is concluded that the effect of the relaxation time on the evolution of the casting process is significant and therefore cannot be neglected.

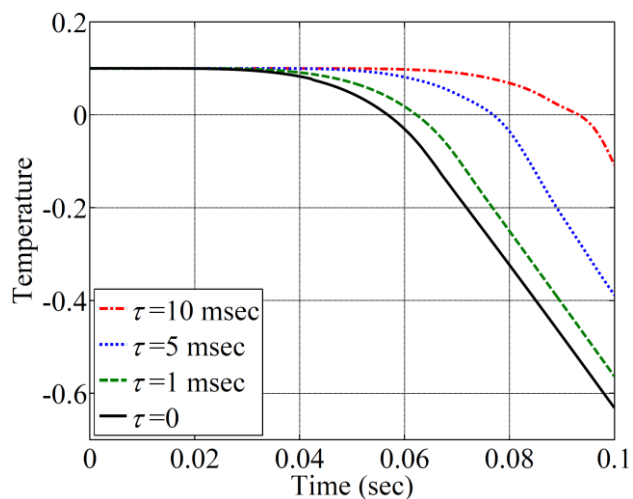


Fig. 7. Time history of temperature at $(x, y) = (0.5, 0.5)$, example 2.

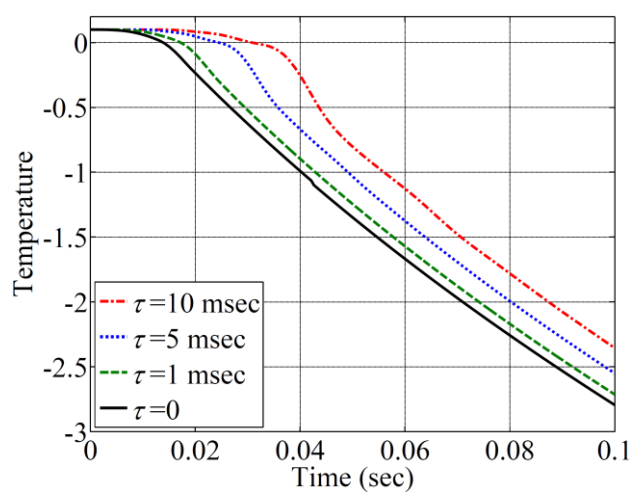


Fig. 8. Time history of temperature at $(x, y) = (0.8, 0.8)$, example 2.

In order to visualize the progress of the solidification process during the time, contours of temperature at different time instances are plotted in Fig. 9. The results shown in this figure correspond to the case with the relaxation time of 10 msec. The isotherms shown in Fig. 8 are computed at time instances of 0.025, 0.05, and 0.1 sec.

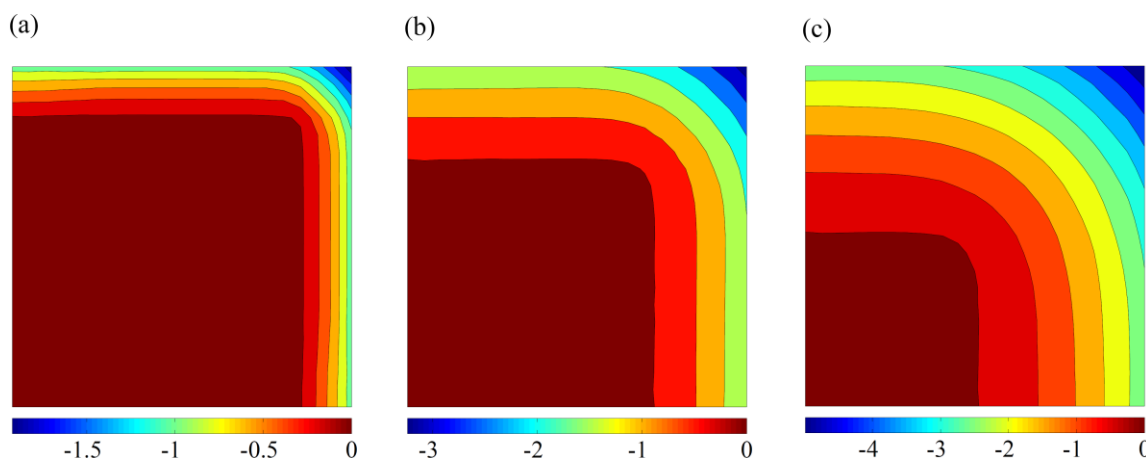


Fig. 9. Contours of temperature at (a) $t = 0.025$ sec, (b) $t = 0.05$ sec, and (c) $t = 0.1$ sec for the continuous casting process with $\tau = 10$ msec.

The position of the solidification front, i.e. the contour of $T = T_s$, at the end of the problem analysis is demonstrated in Fig. 10. In this figure the solidification fronts at $t = 0.1$ sec for different relaxation times are shown. It is clear that as the relaxation time increases the casting process slows down. This means that more time is required to solidify the same amount of material.

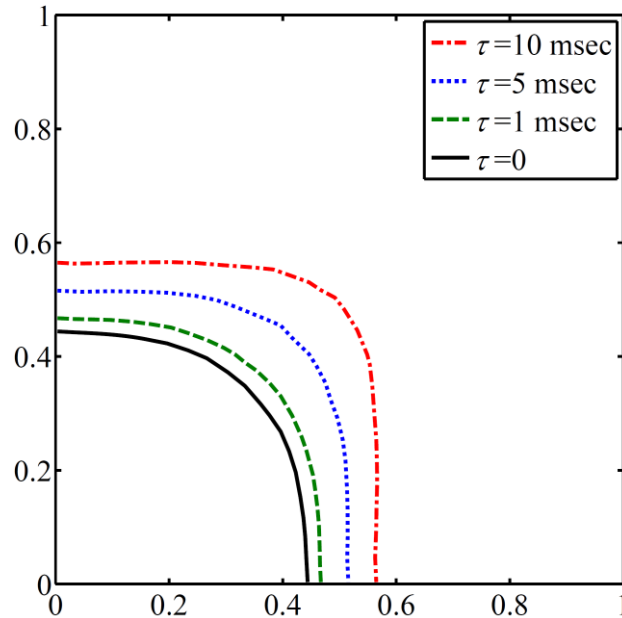


Fig. 10. Position of the solidification front for different values of relaxation time in continuous casting process.

4. Conclusion

In this paper, the effect of finite heat wave speed on the thermal behavior of a solidifying medium was investigated. The meshless RPIM was utilized for the numerical analysis of the Fourier, as well as non-Fourier heat conduction accompanied by phase-change. It was observed that the results of the hyperbolic and parabolic heat conduction equations can be different considering the amount of relaxation time. In general, the following conclusions were drawn:

- Through the numerical examples, it was concluded that the effect of relaxation time is more clearly seen at locations where the heat flux is larger.
- It was also concluded that as the relaxation time increases, so does the delay in the initiation of the solidification at each point.
- The most prominent effect of the hyperbolic heat conduction law is to postpone the initiation of the solidification at each point, i.e., more time is required for each point to solidify.
- The position of the solidification front predicted by the non-Fourier law is always behind of the predictions obtained by the Fourier law.

5. References

- [1] A. Khosravifard and M.R. Hematiyan, Analysis of phase-change heat conduction problems by an improved CTM-based RPIM, *Advances in Boundary Element techniques XIII*, BETEQ 2012, 3-5 September, Prague, (2012).
- [2] R. Vertnik and B. Sarler, Meshless local radial basis function collocation method for convective-diffusive solid-liquid phase change problems, *International Journal of Numerical Methods for Heat & Fluid Flow*, 16 (2006) 617–640.
- [3] G. Kosec and B. Sarler, Solution of phase change problems by collocation with local pressure correction, *CMES: computer Modeling in Engineering and Sciences*, 47 (2009) 191–216.

- [4] R. Vertnik, M. Založnik and B. Sarler, Solution of transient direct-chill aluminium billet casting problem with simultaneous material and interphase moving boundaries by a meshless method, *Engineering Analysis with Boundary Elements*, 30 (2006) 847–855.
- [5] L. Zhang, Y.M. Rong, H.F. Shen and T.Y. Huang, Solidification modeling in continuous casting by finite point method, *Journal of Materials Processing Technology*, 192–193 (2007) 511–517.
- [6] L. Zhang L., H.F. Shen, Y.M. Rong and T.Y. Huang, Numerical simulation on solidification and thermal stress of continuous casting billet in mold based on meshless methods, *Materials Science and Engineering A*, 466 (2007) 71–78.
- [7] G. Zhihua, L. Yuanming, Z. Mingyi, Q. Jilin and Z. Shujuan, An element free Galerkin method for nonlinear heat transfer with phase change in Qinghai–Tibet railway embankment, *Cold Regions Science and Technology*, 48 (2007) 15–23.
- [8] H.S. Fang, K. Bao, J.A. Wei, H. Zhang, E.H. Wu and L. Zheng, Simulations of droplet spreading and solidification using an improved SPH model, *Numerical Heat Transfer, Part A: Applications*, 55 (2009) 124–143.
- [9] M. Zhang, H. Zhang and L. Zheng, Application of smoothed particle hydrodynamics method to free surface and solidification problems, *Numerical Heat Transfer, Part A*, 52 (2007) 299–314.
- [10] H. Yang and Y. He, Solving heat transfer problems with phase change via smoothed effective heat capacity and element free Galerkin methods, *International Communication in Heat and Mass Transfer*, 37 (2010) 385–392.
- [11] M. Alizadeh, S.A. Jenabali Jahromi and S.B. Nasihatkon, Applying finite point method in solidification modeling during continuous casting process, *ISIJ International*, 50 (2010) 411–417.
- [12] G. Kosec and B. Sarler, Meshless Approach to Solving Freezing with Natural Convection, *Materials Science Forum*, 649 (2010) 205–210.
- [13] B. Sarler, G. Kosec, A. Lorbicka and R. Vertnik, A meshless approach in solution of multiscale solidification modeling, *Materials Science Forum*, 649 (2010) 211–216.
- [14] H. Thakur, K.M. Singh and P.K. Sahoo, Phase change problems using the MLPG method, *Numerical Heat Transfer: Part A*, 59 (2011) 438–458.
- [15] G. Kosec, M. Založnik, B. Sarler and H. Combeau, A meshless approach towards solution of macrosegregation phenomena, *Computers, Materials & Continua*, 580 (2011) 1–27.
- [16] S.Y. Reutskiy, The method of approximate fundamental solutions (MAFS) for Stefan problems, *Engineering Analysis with Boundary Elements*, 36 (2012) 281–292.
- [17] R. Vertnik and B. Sarler, Solution of a continuous casting of steel benchmark test by a meshless method, *Engineering Analysis with Boundary Elements*, 45 (2014) 45–61.
- [18] M. Kumar, S. Roy and S.S. Panda, Numerical simulation of continuous casting of steel alloy for different cooling ambiances and casting speeds using immersed boundary method, *Proceedings of the Institution of Mechanical Engineers, Part B: Journal of Engineering Manufacture*, (2015), doi: 10.1177/0954405415596140.
- [19] S.L. Sobolev, The local-nonequilibrium temperature field around the melting and crystallization front induced by picosecond pulsed laser irradiation, *International Journal of Thermophysics*, 17 (1996) 1089–1097.
- [20] A. Vedavarz, K. Mitra and S. Kumar, Hyperbolic temperature profiles for laser surface interactions, *Journal of applied physics*, 76 (1994) 5014–5018.
- [21] D.E. Glass, M.N. Ozisik and S.S. McRae, Formulation and solution of hyperbolic Stefan problem, *Journal of applied physics*, 70 (1991) 1190–1194.
- [22] M.A. Al-Nimr and M.A. Hader, Melting and Solidification under the Effect of the Phase-Lag Concept in the Hyperbolic Conduction Equation, *Heat Transfer Engineering*, 22 (2001) 40–47.
- [23] H. Ahmadikia and A. Moradi, Non-Fourier phase change heat transfer in biological tissues during solidification, *Heat and Mass Transfer*, 48 (2012) 1559–1568.

- [24] A.M. Bakken, Cryopreserving Human Peripheral Blood Progenitor Cells, *Current stem cell research & therapy*, 1 (2006) 47–54.
- [25] C.J. Hunt and P.M. Timmons, Cryopreservation of human embryonic stem cell lines, *Methods in Molecular Biology*, 368 (2007) 261–270.
- [26] N.B. Ishine, C. Rubinsky and Y. Lee, Transplantation of mammalian livers following freezing: vascular damage and functional recovery, *Cryobiology*, 40 (2000) 84–89.
- [27] R.M. Nerem, Tissue engineering: Confronting the transplantation crisis, *Proceedings of the Institution of Mechanical Engineers Part H: Journal of Engineering in Medicine*, 214 (2000) 95–99.
- [28] Siraj-ul-Islam, R. Vertnik and B. Sarler, Local radial basis function collocation method along with explicit time stepping for hyperbolic partial differential equations, *Applied Numerical Mathematics*, 67 (2013), 136–151.
- [29] A. Khosravifard and M.R. Hematiyan, A new method for meshless integration in 2D and 3D Galerkin meshfree methods, *Engineering Analysis with Boundary Elements*, 34 (2010) 30–40.
- [30] A. Khosravifard, M.R. Hematiyan and L. Marin, Nonlinear transient heat conduction analysis of functionally graded materials in the presence of heat sources using an improved meshless radial point interpolation method, *Applied Mathematical Modelling*, 35 (2011), 4157–4174.

تحلیل بدون المان فرآیند ریخته‌گری با در نظر گرفتن انتقال حرارت غیر فوری

امیر خسروی فرد*، محمد رحیم همتیان*
* دانشکده مهندسی مکانیک، دانشگاه شیراز، شیراز، ایران

چکیده: ریخته‌گری بعنوان یکی از فرآیندهای مهم تولید شناخته می‌شود. تحلیل حرارتی یک محیط در حال انجماد برای طراحی مناسب فرآیند ریخته‌گری دارای اهمیت فراوانی است. معادله حاکم متداول یک محیط در حال انجماد بر پایه قانون هدایت حرارت فوری است که در آن، تأخیر زمانی ما بین شار حرارتی و گرادیان دما در نظر گرفته نمی‌شود. در این مقاله، مفهوم تأخیر فاز در پدیده انجماد مورد بررسی قرار می‌گیرد. این مفهوم را با استفاده از معادله هدایت حرارت هذلولوی، که عموماً تحت عنوان معادله ماکسول – کاتانیو شناخته می‌شود، لحاظ می‌کنیم. به این ترتیب، اثر سرعت محدود موج حرارتی بر رفتار حرارتی یک محیط در حال انجماد مورد مطالعه قرار می‌گیرد. در این زمینه، چند مثال عددی توسط روش بدون المان درون‌یابی نقطه‌ای شعاعی تحلیل می‌شود. اثر مدت زمان تأخیر فاز بر رفتار حرارتی محیط در حال انجماد مطالعه می‌شود، همچنین، نتایج معادلات هدایت حرارت فوری و غیر فوری با یکدیگر قیاس می‌گردد. مشاهده می‌شود که با توجه به مسأله خاص انجماد مورد بررسی و نیز مدت زمان تأخیر فاز در نظر گرفته شده، نتایج حاصل از قوانین هدایت حرارت فوری و غیر فوری می‌تواند تفاوت زیادی داشته باشد. مهم‌ترین اثر تأخیر فاز به تعویق انداختن شروع انجماد در هر نقطه است.

کلمات کلیدی: تغییر فاز، هدایت حرارت غیر فوری، روش بدون المان درون‌یابی نقطه‌ای شعاعی